Analytical Methods

PAPER

View Article Online
View Journal | View Issue

Cite this: *Anal. Methods*, 2015, 7, 9785

Effect of fluorescent staining on size measurements of polymeric nanoparticles using DLS and SAXS†

D. Geißler,‡[a] C. Gollwitzer,‡[b] A. Sikora,[c] C. Minelli,[c] M. Krumrey[b] and U. Resch-Genger*[a]

Received 30th July 2015
Accepted 18th October 2015

DOI: 10.1039/c5ay02005k

www.rsc.org/methods

The influence of fluorescence on nanoparticle size measurements using dynamic light scattering (DLS) and small angle X-ray scattering (SAXS) was investigated. For this purpose, two series of 100 nm-sized polymer nanoparticles stained with different concentrations of the fluorescent dyes DY555 and DY680 were prepared, absorbing/emitting at around 560 nm/590 nm and 695 nm/715 nm, respectively. SAXS measurements of these particle series and a corresponding blank control (without dye) revealed similar sizes of all particles within an uncertainty of 1 nm. DLS measurements carried out at three different laboratories using four different DLS instruments and two different laser wavelengths, *i.e.*, 532 nm and 633 nm, revealed also no significant changes in size (intensity-weighted harmonic mean diameter, *Z*-Average) and size distribution (polydispersity index, PI) within and between the two dye-stained particle series and the blank sample. Nevertheless, a significant decrease of the detected correlation coefficients was observed with increasing dye concentration, due to the increased absorption of the incident light and thus, less coherent light scattering. This effect was wavelength dependent, *i.e.* only measurable for the dye-stained particles that absorb at the laser wavelength used for the DLS measurements.

Introduction

Fluorescent nanoparticles such as dye-stained polymer particles, dye-labelled silica-particles and semiconductor quantum dots are increasingly used as reporters in various bioanalytical applications for *in vivo* and *in vitro* spectroscopy and imaging.[1–7] Particle size is a key parameter that determines the behavior and colloidal stability of particle reporters and their interaction with biological systems together with the surface chemistry (*i.e.* number of functional groups at the surface) and particle charge.[8,9]

Two commonly used techniques to determine the sizes of nanoparticles are dynamic light scattering (DLS), available in many different laboratories preparing or working with nanoparticles, and the more sophisticated small angle X-ray scattering (SAXS), that can be made traceable to the International System of Units (SI).[10] Whereas SAXS depends on the scattering of X-rays based upon the electron density of the particles, which should be independent of any fluorescence signals, DLS relies on light scattering and may thus be affected by the absorption and emission of labelled dyes or self-luminescent nanomaterials. Depending on the optical properties and the wavelength of the laser used for the DLS measurements, absorption can result in a partial loss of the coherent incident light and the subsequently emitted non-coherent fluorescence may also affect the measured signal. Moreover, strong absorption can cause unwanted side effects such as local sample heating, beam expansion, and convection, that interfere with the sample characterization.[11] Thus, DLS measurements of strongly absorbing samples and highly turbid colloidal systems can be challenging. To overcome the limitations of common DLS, modified and improved optical scattering techniques have been developed, such as 3D cross-correlation DLS,[12–15] DLS using a flat cell light scattering instrument,[16] diffusing wave spectroscopy,[17] or photon density wave spectroscopy.[18,19] However, many researcher that work with fluorescent nanoparticles for bioanalytical applications still use common DLS systems to characterize their particle samples, due to the wide availability and broad application range of this established technique.

There are several publications on the comparison of DLS and SAXS size measurements for different particle systems such as micelles, proteins, and polymers.[20–25] However, until today there exists no systematic investigation on the influence of fluorescence on these particle size measurement techniques.

[a]*Federal Institute for Materials Research and Testing (BAM), Richard-Willstätter-Str. 11, 12489 Berlin, Germany. E-mail: ute.resch@bam.de*

[b]*Physikalisch-Technische Bundesanstalt (PTB), Abbestr. 2-12, 10587 Berlin, Germany*

[c]*National Physical Laboratory (NPL), Hampton road, TW11 0LW, Teddington, UK*

† Electronic supplementary information (ESI) available: A comparison of the SAXS fits assuming either solid spherical particles or core–shell particles (Fig. S1), the emission spectra of the dye-stained particles (Fig. S2), examples for the model fit of the SAXS scattering curves and the corresponding fit results (Fig. S3), the polydispersity index (PI) values measured with DLS (Fig. S4), as well as the number-weighted sizes and size distributions measured with DLS (Fig. S5). See DOI: 10.1039/c5ay02005k

‡ Both authors equally contributed to the manuscript.

This encouraged us to systematically assess the influence of the optical properties on both types of size measurements. For this purpose, two series of dye-stained polymer particles were prepared using two fluorescent dyes absorbing and emitting at different wavelength, covering the laser wavelengths of typical DLS setups, *i.e.*, 532 nm and 633 nm, and characterized them regarding their particle size and size distribution. Based upon these results, possible limitations of DLS techniques are derived.

Experimental

Materials

Carboxyl-functionalized polystyrene nanoparticles with 105 nm nominal diameter (batch # GKCML927W) were purchased from Kisker Biotech GmbH. The particles were treated with ultrasound prior to use. The fluorescent dyes DY555 (batch # E17-03077) and DY680 (batch # E08-13087) were purchased as carboxylic acid modifications from Dyomics GmbH and were employed without further purification. UV-spectroscopic grade dimethylformamide (DMF) was obtained from Sigma-Aldrich Co.

Methods

Preparation of dye-stained polymer particles. Carboxylated polystyrene (PS) particles with a nominal size of 105 nm were stained with the hydrophobic fluorescent dyes DY555 or DY680 using a modified swelling/de-swelling procedure developed by Behnke *et al.*[26,27] The precursor PS particles were diluted with ultrapure water (MilliQ) to yield 10 mg mL^{-1} particle dispersions. Two fluorescent dye stock solutions with a concentration of 1 mM were prepared by dissolving 0.4 mg of each solid dye in 630 μL DMF. By further diluting these solutions by factors of 1 : 2, 1 : 5, and 1 : 10 with DMF, additional concentrations comprising 0.5 mM, 0.2 mM and 0.1 mM dye solutions were obtained. Staining was performed by adding 200 μL of a dye solution to 1200 μL PS particle dispersion in Eppendorf tubes. The resulting dye/particle mixtures in water/DMF (6 : 1) were incubated for 30 min (with shaking) at room temperature. Each staining mixture was than divided into two 700 μL aliquots and centrifuged for 45 min at 17 500*g* using an Eppendorf 5424R centrifuge. After centrifugation, the supernatant was removed, 1 mL ultrapure water was added to each tube, and the pellet was dispersed using ultrasound and vortexing. Washing with ultrapure water was repeated twice for a total of three washing cycles. At the final step, only 600 μL of ultrapure water was added. Finally, each of the two 600 μL aliquots of the same kind were combined to yield 1.2 mL of dye-stained PS particle dispersions with a concentration of 10 mg mL^{-1} that are stained with either 0.1 mM, 0.2 mM, 0.5 mM or 1.0 mM DY555 or DY680. In summary, eight different dye-loaded samples were prepared plus a blank that underwent all washing steps except for the actual staining (pure DMF was used instead).

Instrumentation

Absorption and emission spectroscopy. Absorption spectra were recorded on a calibrated CARY 5000 spectrophotometer (Varian Inc., Palo Alto, USA). The emission spectra were measured with a calibrated Edinburgh Instruments FLS spectrofluorometer (Edinburgh Instruments, Livingston, UK). All absorption and emission measurements were performed with air-saturated solutions at $T = (25 \pm 1)$ °C using 10 mm × 10 mm quartz cuvettes from Hellma GmbH (Müllheim, Germany).

Dynamic light scattering (DLS). The DLS experiments were carried out in three different laboratories using Zetasizer Nano instruments (Malvern Instruments, Worcestershire, UK). Zetasizers equipped with either a "red" 633 nm He–Ne laser or a "green" 532 nm argon laser were used to check for instrument-to-instrument variations as well as for the influence of different laser wavelengths. In a standard DLS measurement, measuring each sample three times with 15 runs per measurement and 15 seconds per run, not all runs are used for the final calculation of the size and size distribution. A distinct fraction of runs is removed from the final measurement calculation by a dust filtration algorithm integrated into the instrument's software (*e.g.*, runs with larger intensity fluctuation due to dust particles or particle agglomerates within the focus distort the measurement). Thus instead of these settings, each sample was measured 100 times with a single run per measurement and a detection period of 10 seconds per run, to ensure that every single measurement run is recorded and can be used to detect possible effects of fluorescence staining on DLS size measurements. For the DLS measurements, the dye-stained particle samples were diluted with ultrapure water (MilliQ) to a final concentration of 0.1 g L^{-1} in disposable low volume cuvettes. All samples were measured at a scattering angle of 173° (backscatter) using the "General purpose" analysis model and the default size analysis parameters as well as a refractive index of 1.59 for the polystyrene particle matrix as sample parameter.

As all dye-stained particle samples displayed monomodal and monodisperse size distributions, the results of the cumulant fits, namely the intensity-weighted harmonic mean particle diameter (*Z*-Average) and the polydispersity index (PI) according to ISO 22412,[28] were used to compare sizes and size distributions of the different samples. Grubb's test was carried out to detect any outliers within the 100 recorded data points, and the mean values and standard deviations were then calculated from the remaining data points (without outliers).

Small angle X-ray scattering (SAXS). The SAXS experiments were performed at the four-crystal monochromator (FCM) beam line of PTB at the synchrotron radiation facility BESSY II in Berlin.[29] The samples in suspension were filled into disposable glass capillaries which are made of borosilicate glass with an inner diameter of 1 mm and a wall thickness of 10 μm. The capillaries were closed by welding the upper end in the flame of a propane/oxygen torch and then placed into a sample holder. This holder was mounted on a six axes manipulator in a high vacuum chamber. The synchrotron radiation was collimated using pinholes to a size smaller than 0.5 × 0.5 mm^2 and focused on the sample. The incident photon flux was measured using a thin photodiode in transmission located upstream after the beam-defining pinhole and before the anti-scatter guard pinhole. A removable, calibrated diode behind the sample was used to measure the transmission of the sample. The scattered

radiation was collected by a vacuum-compatible PILATUS 1 M detector at a distance of (4534.7 ± 0.5) mm behind the sample.[30] The measurements were performed at a photon energy E of (8000 ± 0.8) eV. Each sample was recorded for an integration time of 300 s in 5 rounds, for a total exposure time of 1500 s for each sample.

The scattering curves were obtained by circular integration of the scattering pattern and show the scattered intensity as function of the momentum transfer q which is calculated according to $q = (4\pi E/hc)\sin\theta$ where θ is half of the scattering angle, h is the Planck constant and c is the speed of light. All curves were normalized by incident flux, exposure time and sample transmission. A model equation describing polydisperse spherical particles with a core–shell structure and a Gaussian size distribution was fitted to the data using least-squares adjustment. The core–shell form factor is necessary to fit the scattering data because the carboxylated polystyrene nanoparticles used are coated with a thin PMMA shell. This was shown before using contrast variation SAXS[31] and XPS,[25] and a comparison of the SAXS fits assuming either solid spheres or core–shell particles are displayed in Fig. S1 in the ESI.† The staining did not change the structure further as seen by SAXS. An additive background comprising a constant intensity, a power-low decay and a linear term was assumed. The uncertainty contribution of this model fitting to the number-weighted mean particle diameter was estimated from the residual sum of squares χ^2 by finding the deviation from the best fit diameter at which χ^2 exceeds $2\chi_{min}{}^2$.[10]

Results and discussion

In order to investigate the effect of fluorophore staining on particle size measurements with DLS and SAXS, nanoparticles stained with two different fluorescent dyes were tested, absorbing at either one of the laser wavelengths commonly used for DLS measurements. The absorbance spectra of the DY555- and DY680-stained nanoparticles are shown in Fig. 1. The applied staining concentrations are chosen to be representative for many commercial fluorescent dye-labelled or -stained particles used in various bioanalytical applications. The DY555-stained particles absorb at 532 nm and are thus electronically excited, yet not at 633 nm, whereas the DY680-stained particles absorb at 633 nm, but not at 532 nm.

The measured SAXS curves of the samples are displayed in Fig. 2. As to be expected, the scattering curves do not show differences in the frequency of the oscillations for the differently strained particles and match with the curve obtained for the blank sample.

The scattering curves were fitted with a model equation describing polydisperse spherical core–shell particles having a Gaussian size distribution. Fig. 3 displays the mean diameters of the samples with the model uncertainty as defined above. The best fit diameters are significantly different from the mean values defined by the boundaries for which $\chi^2 > 2\chi_{min}{}^2$ (*cf.* ESI, Fig. S3†), which means that there is a strong correlation between the particle diameter with other adjustable parameters of the model leading to larger uncertainties. However, all values

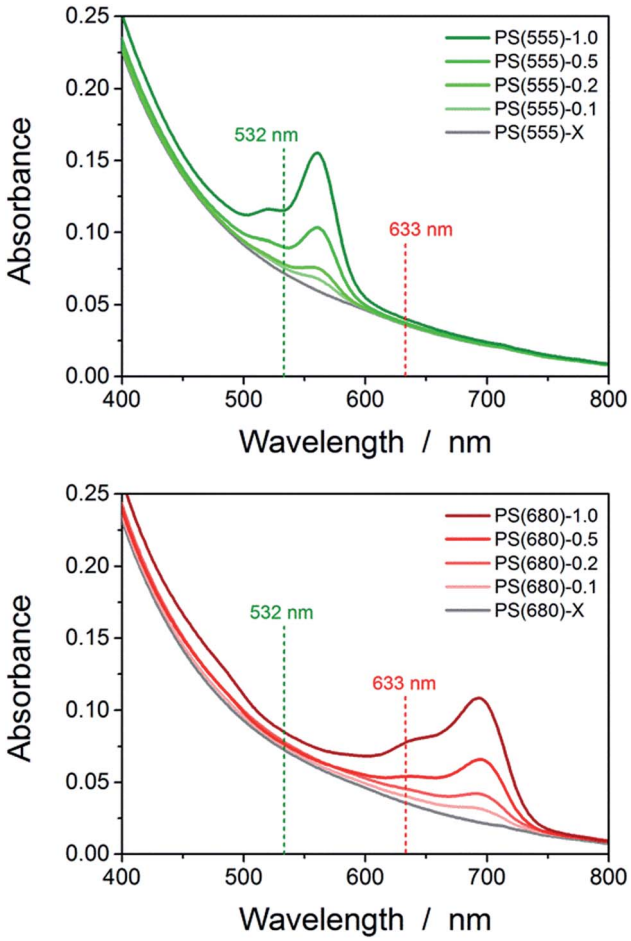

Fig. 1 Absorbance spectra of the DY555-stained (top) and DY680-stained (bottom) nanoparticles doped with different dye concentrations (0.1, 0.2, 0.5, and 1.0 mM) as well as the blank/control particles treated with DMF only (*X*). The absorption of the sterically incorporated dyes is superimposed on the scattering of the 100 nm-sized particles. The dotted lines indicate the laser wavelengths of the different Zetasizer instruments, *i.e.*, 532 nm (green) or 633 nm (red). The corresponding emission spectra of the dye-stained particles are shown in Fig. S2 in the ESI.†

agree within the stated standard uncertainty and there is no significant difference. Due to the fact that the particles were all prepared from the same precursor material and treated in a very similar manner, therefore having a very similar size distribution and inner structure, these values can also be compared within the uncertainty given by the reproducibility of SAXS measurements.

The fits of the SAXS curves reveal a mean diameter of (102 ± 6) nm for all particles with a size distribution of 6.7% CV (SD/mean), which corresponds to a full width at half maximum (FWHM) of 16 nm, *i.e.* a size distribution (FWHM/mean) of 16%.

The reproducibility was determined by measuring the precursor material three times over a course of two years, with a variation of the resulting best fit diameter below 1 nm. Even within this reduced uncertainty all diameters of the dye loaded particles agree. It can be concluded that the particle diameter does not change by more than 1 nm by the dye staining. The

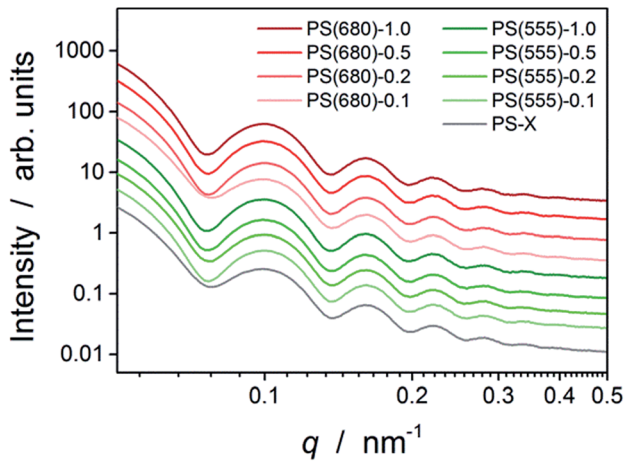

Fig. 2 SAXS curves for the DY555-stained (green curves) and DY680-stained (red curves) nanoparticle samples, as well as for the blank (unstained) control particles (grey curve). The scattering intensities of all particle samples are in fact very similar, but were shifted for better visualization.

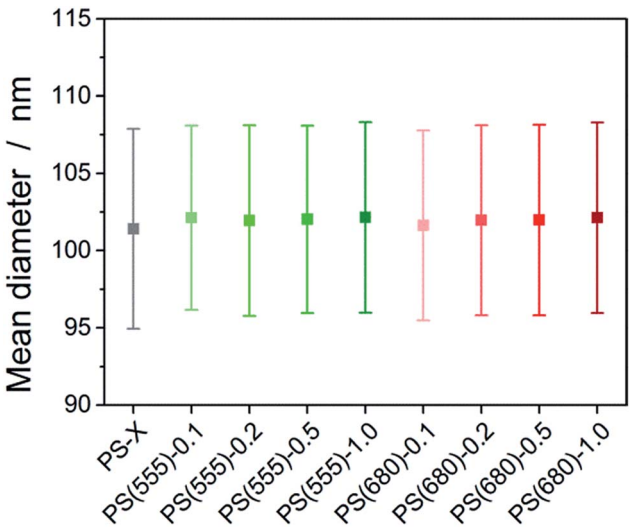

Fig. 3 Size measurement results for the dye-stained nanoparticle samples as measured with SAXS. The colored squares and bars represent the mean diameters and standard uncertainties, respectively.

presence of the fluorophore does also not significantly influence the SAXS measurements. Therefore, the particle diameter as determined by SAXS is a robust measure also in the presence of fluorophore labelling or staining.

The cumulant fit results of the DLS measurements of the different dye-stained particles measured with different Zetasizer instruments are displayed in Fig. 4 (the respective size distributions are shown in Fig. S4 within the ESI†).

Neither the measured particle sizes (*Z*-Average values, Fig. 4) nor the measured size distributions (PI values, Fig. S4 in the ESI†) show a significant change or trend compared to the other particles (blank or dye-stained) for the DLS studies. Obviously, the measured sizes and size distributions are independent of the Zetasizer instrument and/or the operator (similar results obtained in all laboratories), the dye absorption wavelength (similar results for DY555- and DY680-stained particles) or the dye staining concentration (similar results for all particles of a staining series with dye concentrations ranging from 0 to 1 mM), if the same type of DLS instrument is used. Moreover, Fig. 4 reveals that no significant size differences were detected between and within the two different-particle series at different laser wavelength, although DY555 absorbs at 532 nm, whereas DY680 absorbs at 633 nm. This confirms that there is no significant effect of the dye absorption wavelength or dye staining concentration on measured sizes, regardless of the laser wavelengths used.

The mean diameters of (118 ± 1) nm obtained with the cumulant DLS method are considerably larger than the (102 ± 6) nm as measured with SAXS, because DLS measures the hydrodynamic size including an electrochemical double layer, whereas SAXS detects the electron density and thus, the "real" physical sizes of the particles. Moreover, the *Z*-Average

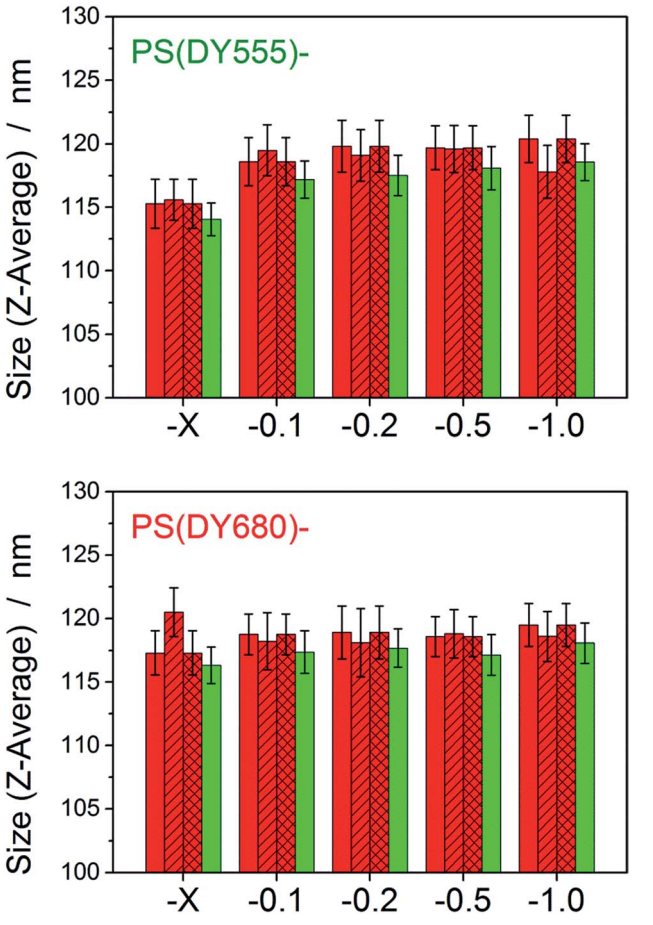

Fig. 4 Size measurement results (*Z*-Average values) of the DY555-stained (top) and DY680-stained (bottom) PS particles as measured with DLS using either a "red" 633 nm laser (red bars) or a "green" 532 nm laser (green bars). The different textures of the red bars indicate measurements carried out at three different laboratories, and the error bars denote the standard deviations of the mean of the 100 measurements after outlier removal. The measured *Z*-Average values reveal no significant effect of the dye absorption wavelength or dye staining concentration.

values reported for DLS are intensity-weighted harmonic mean diameters, whereas the mean diameters determined by SAXS are based on a number-weighted size distribution (*i.e.* assuming a Gaussian number distribution of the particle sizes). However, the polydispersity index of PI = 0.04 obtained with DLS for all samples correspond to a FWHM of 24 nm, *i.e.* a size distribution of 20% (FWHM/mean). This value agrees with the SAXS result (16%), and with previous investigations applying differential centrifugal sedimentation (DCS), where a mean hydrodynamic particle diameter of 124 nm and a FWHM of 15 nm (FWHM/mean of 12%) was obtained.[25] Moreover, the number-weighted sizes and size distributions obtained with the non-negative least square (NNLS) algorithm for DLS (Fig. S5 in the ESI†) reveal a mean particle diameter of (99 ± 4) nm for all samples with a size distribution of (24 ± 1) nm, which again corresponds well with the SAXS results.

Although no significant change or trend was observed with DLS on the sizes and size distribution of the dye-stained particles, the dye absorption wavelength and staining concentration, however, have a significant influence on the intercepts of the correlation functions at small correlation times. This is displayed in Fig. 5.

The intercepts of the correlations functions in Fig. 5 reveal a clear wavelength-dependence, *i.e.*, a dependence on the absorption and emission properties of the fluorescent dye used for particle staining. Whereas for the DY555-stained particles, the correlation function intercepts show a significantly decrease with increasing DY555 staining concentration with the "green" laser (Fig. 5, top left), no influence is measured with the "red" laser (Fig. 5, top right). In contrast, the correlation function intercepts for the DY680-stained particles are identical when recorded with the "green" laser (Fig. 5, bottom left), but decrease with increasing DY680 staining concentration for the "red" laser (Fig. 5, bottom right). Hence, the intercepts of the correlations functions are clearly affected if the dye absorbs at the laser wavelength, as in this case, the absorption of the incident light reduces the number of scattered photons compared to non-absorbing particles, leading to an inherent loss in sensitivity. The size of this loss correlates with the number of absorbed photons and hence, with the absorption cross section of the particles and their number concentration. If these particles are also fluorescent, the accordingly emitted photons, that are non-coherent in contrast to the scattered photons, are detected as baseline noise in the correlogram measured in the DLS experiment, thereby reducing the data quality.[32] Nevertheless, it has been shown that the nanoparticle size determination with DLS in a standard configuration is not affected by dye-staining if the fluorophore concentration remains reasonably low, while the correlation functions are already clearly changed. Dependent on the type of incorporated dye, higher staining concentrations can induce fluorescence quenching due to dye–dye interactions, thereby diminishing the emission intensities of the fluorescent particles[27] (see also the emission spectra of the particles in the ESI, Fig. S2†). However, for significantly higher dye concentrations, or particles with extremely high extinction coefficients such as quantum dots, DLS measurements are still possible by adding bandpass filters in front of the detector to discriminate the (undesired) fluorescence photons from scattered photons.[32]

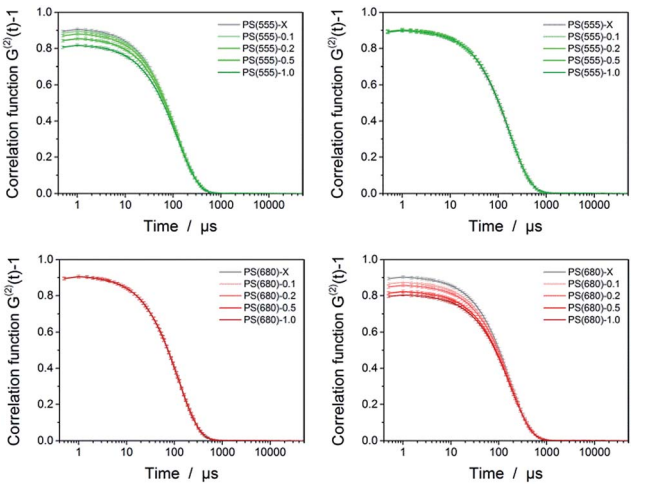

Fig. 5 Intensity autocorrelation functions $G^{(2)}(t) - 1$ as measured with DLS for the DY555-stained (top) and DY680-stained (bottom) PS particles with a "green" 532 nm laser (left) and with a "red" 633 nm laser (right).

Conclusions

The influence of absorption and fluorescence on dynamic light scattering (DLS), one of the most common laboratory method to characterize all types of nanoparticles, and on small angle X-ray scattering (SAXS) size measurements was studied using two series of dye-stained polymer nanoparticles. SAXS, as traceable method for nanoparticle size determination, is not affected by fluorescence, and could be thus used to verify the independence of nanoparticle size on the encapsulation procedure employed for particle staining, and the fluorophore concentration. DLS revealed also no significant influence of absorbing and emitting dyes as confirmed by the barely affected particle size (*Z*-Average) and size distribution (polydispersity index PI) within and between the two dye-stained particle series and the blank sample measured with different laser excitation wavelengths. Moreover, the DLS results were independent of the instrument/operator (different Zetasizers in different laboratories). DLS provides reliable size measurements even of fluorescent nanoparticles if their emission is reasonably low. For highly fluorescent particles, a significant decrease of the correlation coefficients is observed due to the increased absorption of the coherent incident light. Together with the corresponding emission of non-coherent fluorescence light, this results in a reduced data quality. For the reliable size measurement of strongly emitting particles, it is recommended to include a bandpass filter in front of the DLS detector to remove fluorescence photons. The loss in scattering photons by strong absorption of the incident laser light can be best compensated for by more repetitions as an increase in particle concentration may favor particle aggregation.

Acknowledgements

We thank Prof. Dr Rainer Haag (FU Berlin) for permission to use their Malvern Zetasizers and Dr Emanuel Fleige (FU Berlin, DendroPharm GmbH) for assistance during the DLS measurements. We thank Dr Ben MacCreath (Malvern Instruments Ltd.) for fruitful discussions regarding DLS on fluorescent samples. We gratefully acknowledge financial support from the European Commission (EMRP project NEW03 NanoChOp). The EMRP is jointly funded by the EMRP participating countries within EURAMET and the European Union.

Notes and references

1 H. Goesmann and C. Feldmann, *Angew. Chem., Int. Ed.*, 2010, **49**, 1362.
2 X. X. He, K. M. Wang and Z. Cheng, *Wiley Interdiscip. Rev.: Nanomed. Nanobiotechnol.*, 2010, **2**, 349.
3 R. G. Chaudhuri and S. Paria, *Chem. Rev.*, 2012, **112**, 2373.
4 F. P. Zamborini, L. L. Bao and R. Dasari, *Anal. Chem.*, 2012, **84**, 541.
5 R. A. Sperling and W. J. Parak, *Therapeutic Innovation & Regulatory Science*, 2013, **47**, 1333.
6 P. D. Howes, R. Chandrawati and M. M. Stevens, *Science*, 2014, **346**, 1247390.
7 E. Petryayeva and W. R. Algar, *RSC Adv.*, 2015, **5**, 22256.
8 K. E. Sapsford, K. M. Tyner, B. J. Dair, J. R. Deschamps and I. L. Medintz, *Anal. Chem.*, 2011, **83**, 4453.
9 K. E. Sapsford, W. R. Algar, L. Berti, K. B. Gemmill, B. J. Casey, E. Oh, M. H. Stewart and I. L. Medintz, *Chem. Rev.*, 2013, **113**, 1904.
10 F. Meli, T. Klein, E. Buhr, C. G. Frase, G. Gleber, M. Krumrey, A. Duta, S. Duta, V. Korpelainen, R. Bellotti, G. B. Picotto, R. D. Boyd and A. Cuenat, *Meas. Sci. Technol.*, 2012, **23**, 125005.
11 W. Schärtl, *Light Scattering from Polymer Solutions and Nanoparticle Dispersions*, Springer-Verlag, Berlin, Heidelberg, 2007.
12 K. Schatzel, M. Drewel and J. Ahrens, *J. Phys.: Condens. Matter*, 1990, **2**, Sa393.
13 K. Schatzel, *J. Mod. Opt.*, 1991, **38**, 1849.
14 C. Urban and P. Schurtenberger, *J. Colloid Interface Sci.*, 1998, **207**, 150.
15 M. Medebach, N. Freiberger and O. Glatter, *Rev. Sci. Instrum.*, 2008, **79**, 073907.
16 M. Medebach, C. Moitzi, N. Freiberger and O. Glatter, *J. Colloid Interface Sci.*, 2007, **305**, 88.
17 D. J. Pine, D. A. Weitz, P. M. Chaikin and E. Herbolzheimer, *Phys. Rev. Lett.*, 1988, **60**, 1134.
18 R. Hass and O. Reich, *ChemPhysChem*, 2011, **12**, 2572.
19 L. Bressel, R. Hass and O. Reich, *J. Quant. Spectrosc. Radiat. Transfer*, 2013, **126**, 122.
20 J. Wagner, W. Hartl and R. Hempelmann, *Langmuir*, 2000, **16**, 4080.
21 L. Galantini, E. Giglio, A. Leonelli and N. V. Pavel, *J. Phys. Chem. B*, 2004, **108**, 3078.
22 A. F. Thünemann, P. Knappe, R. Bienert and S. Weidner, *Anal. Methods*, 2009, **1**, 177.
23 T. Sato, T. Fukasawa, K. Aramaki, O. Glatter and R. Buchner, *J. Mol. Liq.*, 2011, **159**, 76.
24 C. J. Kim, K. Sondergeld, M. Mazurowski, M. Gallei, M. Rehahn, T. Spehr, H. Frielinghaus and B. Stuhn, *Colloid Polym. Sci.*, 2013, **291**, 2087.
25 C. Minelli, R. Garcia-Diez, A. E. Sikora, C. Gollwitzer, M. Krumrey and A. G. Shard, *Surf. Interface Anal.*, 2014, **46**, 663.
26 T. Behnke, C. Würth, K. Hoffmann, M. Hubner, U. Panne and U. Resch-Genger, *J. Fluoresc.*, 2011, **21**, 937.
27 T. Behnke, C. Würth, E. M. Laux, K. Hoffmann and U. Resch-Genger, *Dyes Pigm.*, 2012, **94**, 247.
28 International Standard ISO 22412, *Particle size analysis – Dynamic light scattering (DLS)*, International Organization for Standardization (ISO), ISO/TC 24/SC 4, 2008.
29 M. Krumrey and G. Ulm, *Nucl. Instrum. Methods Phys. Res., Sect. A*, 2001, **467**, 1175.
30 J. Wernecke, C. Gollwitzer, P. Muller and M. Krumrey, *J. Synchrotron Radiat.*, 2014, **21**, 529.
31 R. Garcia-Diez, C. Gollwitzer and M. Krumrey, *J. Appl. Crystallogr.*, 2015, **48**, 20.
32 Application of Dynamic Light Scattering (DLS) to Protein Therapeutic Formulations, *Principles, Measurements and Analysis 4. FAQs*, Malvern Instruments Limited, 2015.

